Applied Energy 133 (2014) 80–88

Contents lists available at ScienceDirect

Applied Energy

journal homepage: www.elsevier.com/locate/apenergy

Theoretical limits of thermoelectric power generation from exhaust gases

Robert J. Stevens [a,*], Steven J. Weinstein [b], Karuna S. Koppula [b]

[a] Department of Mechanical Engineering, Rochester Institute of Technology, 76 Lomb Memorial Drive, Rochester, NY 14623, USA
[b] Department of Chemical Engineering, Rochester Institute of Technology, 160 Lomb Memorial Drive, Rochester, NY 14623, USA

HIGHLIGHTS

- Variational method is used to optimize thermal system.
- Theoretical limit for thermoelectric power generation from exhaust is established.
- Thermoelectric figure of merit alone is not sufficient to predict system efficiency.
- Four modeling approach for thermoelectric optimization are compared.
- Wiring thermoelectric leg pairs in series versus parallel results in higher power.

ARTICLE INFO

Article history:
Received 21 April 2014
Received in revised form 18 July 2014
Accepted 19 July 2014
Available online 12 August 2014

Keywords:
Waste heat recovery
Thermoelectric
Variational method
TEG
Power generation
Optimization

ABSTRACT

The recovery of energy from exhaust gases using thermoelectric generators is of growing interest. The electrical loading of the thermoelectric system impacts the amount of energy that can be recovered. This paper presents a model for the theoretical limit of electrical power generation that provides optimal electrical loading conditions for a given exhaust stream and system configuration. The analysis of a sample heat recovery configuration indicates that the simple isothermal modeling approach often applied to individual thermoelectric leg pairs is not sufficient to optimize power generation when a significant amount of energy is removed from the exhaust stream via a sequence of leg pairs. The analysis establishes that ZT, the thermoelectric figure of merit, is not a sufficient metric to describe system level performance. The analysis predicts that there is an optimum number of thermoelectric leg pairs that maximize the power extracted for any system, and that adding more leg pairs beyond this optimum can degrade system performance. The theoretical limit for power generation is compared to proposed electrically loading strategies found in the literature. The developed model has low computational load and is suitable for use in system optimization models.

1. Introduction

The growing need for electricity, and the heightened concern about environmental issues associated with traditional energy generating technologies, has increased interest in the use of thermoelectrics to directly convert thermal energy into electrical energy. Thermoelectrics may enable a viable pathway for capturing waste heat, and may be integrated with other power cycles to improve overall efficiency and reduce costs. There is substantial interest in utilizing thermoelectric devices for automobile exhaust-to-electricity conversion [1]. According to a recent Department of Energy Industrial Technology Program study [2], the waste energy equivalent to 1.72 billion barrels of oil is lost each year in the United States industrial sector alone. Significant energy savings may be achieved by recovering even a small portion of this discarded thermal energy. Thermoelectrics have some distinct advantages since they are modular, have no moving parts, and are able to operate over a wide range of transient temperature conditions. High costs and poor efficiencies, however, have deterred a more rapid adoption of thermoelectric devices.

There have been significant advancements in thermoelectric material properties in recent years [3,4]. Optimization of a single leg pair to extract the most waste energy has been well established by altering material properties and leg geometry [5]. The use of functionally graded materials or the stacking of leg materials has also been considered to optimize individual devices [6,7]. However, the optimal conditions at which to operate a single leg pair

* Corresponding author.
E-mail address: rjseme@rit.edu (R.J. Stevens).

http://dx.doi.org/10.1016/j.apenergy.2014.07.075
0306-2619/

Nomenclature

A	cross sectional area of a leg (m^2)
b	length of a leg pair including open space between legs (m)
C	coefficients used to simplify expressions
c_p	specific heat (J/kg K)
D	coefficients used to simplify expressions
I	current (A)
j	current flux (A/m^2)
k	thermal conductivity (W/m K)
K	thermal conductance of a leg pair (W/K)
l	height of a leg (m)
L	system length (m)
m	ratio of electrical load to internal resistance for local efficiency optimization ()
$\dot{m}$	mass flow rate (g/s)
N	number of leg pairs ()
P	system electric power generation (W)
q	heat rate of a leg pair (W)
Q	system heat transfer rate (W)
R	overall thermal resistances between the fluids and thermoelectric junction for a single leg pair (K/W)
R_c''	thermal contact resistance ($K\ m^2/W$)
R_e	electrical resistance of a leg pair (Ω)
T	temperature (K)
$\overline{T}$	average of hot and cold side leg temperature (K)
T^*	integral average voltage difference across leg pairs for entire system (K)
$T_{ambient}$	sink temperature (K)
V	voltage across leg pair (V)
w	width of a thermoelectric leg pair couple including open space between legs (m)
x	distance from leading inlet of system (m)
z	thermoelectric figure of merit (1/K)

Greek symbols

α	Seebeck coefficient (V/K)
η	efficiency of a thermoelectric leg pair
η_{sys}	system efficiency
λ	Lagrange multipliers
ρ	electrical resistivity (Ω cm)
ψ	function to be optimized

Subscripts

1-6	constants index
c	thermal contact
h,c	hot and cold side
i,o	inlet and outlet of system
p,n	p and n type legs

Superscripts

$''$	on area basis

does not necessarily apply to a sequence of leg pairs, especially when the temperature of the heat source and/or sink changes appreciably along the system. This is not surprising, since energy removal by a single leg pair affects the temperature field for subsequent leg pairs, and the interaction between these leg pairs is thus nontrivial.

Miller et al. modeled a thermoelectric system with an organic Rankine bottoming cycle for heat recovery from exhaust heat [8]. The model accounted for the effects of various design parameters and the thermal resistance of the heat exchanger surfaces. The model assumes an isothermal surface, which is applicable only if a small fraction of the available energy is extracted from the exhaust heat. The isothermal assumption has been used in modeling waste heat recovery and solar thermal cycles [9,10].

Gao et al. developed a model of a sequence of thermoelectric modules in a counter flow to recover waste energy from a PEM fuel cell [11]. The model enabled each module, a discrete device with a multiple leg pairs wired electrically in series, to either operate electrically in series or in stand-alone mode. For the stand-alone mode, the applied electrical load across a module was set to equal the internal electrical resistance of the module. Although this approach will naturally guarantee that the power will be maximized for a given temperature difference across a single leg pair, the approach will not necessarily generate the maximum power for the entire system. Zhou et al. implemented a multi-scale thermoelectric model that also matched the external load with the internal electrical resistance, and explored the impact of a range of design parameters and flow conditions on pressure drop and power generation [12]. Yu and Zhao and Kumar et al. also considered legs in series and the load resistance was selected to equal that of the effective internal resistance of the modules [13–15].

Crane developed a numerical model for multiple leg pairs and used a MATLAB function to iteratively optimize each element efficiency for an automobile exhaust recovery system [16]. The legs operated electrically in series. Crane's approach adjusted the total load resistance in order to optimize overall power generation as opposed to the approach of load matching typically done with a single module (a discrete device with multiple leg pairs in series). He validated the model experimentally for a small system. Wang et al. used a numerical approach to optimize a thermoelectric generator coupled to vehicle exhaust, and found that the optimal power is reached when the applied electrical resistance is greater than the internal resistance for cases where all leg pairs are in series [17].

Liang et al. used a slightly different approach to optimize a sequence of thermoelectric modules by fixing the voltage across parallel strings of thermoelectric legs pairs [18]. Min and Rowe [19] assumed that the optimal operation occurs when all leg pairs individually operate at peak efficiency as defined by Ioffe [20].

The above-cited literature indicates that the electrical loading of a sequence of thermoelectric elements has an impact on system overall performance. The purpose of this paper is to develop a theoretical limit for the amount of power that can be recovered from an exhaust gas. This limit is extracted from a model of low computational load, so it is suitable for use to optimize large systems. The results of this theoretical limit model are compared to alternative

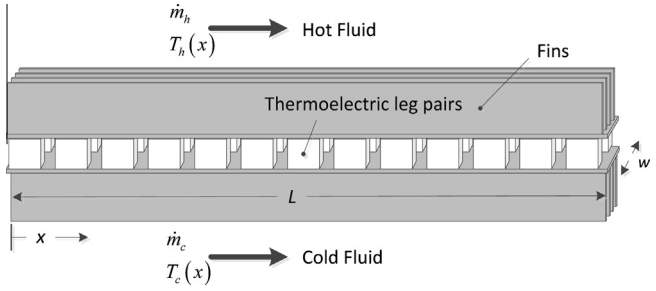

Fig. 1. Schematic of thermoelectric power generation system.

approaches to optimization, some of which have been cited above. In particular, we compare our approach and results for the following cases: (i) the local efficiency of each leg pair is optimized, (ii) a constant voltage is applied across all leg pairs, and (iii) a constant current is applied across all leg pairs.

2. Thermal model

A schematic of the waste heat thermoelectric power generator to be modeled is shown in Fig. 1. This structure is typical of many waste heat recovery systems. A hot fluid flows across a surface, which is in thermal contact with multiple thermoelectric leg pairs. The underside of these thermoelectric leg pairs are cooled by coolant passing across a surface in thermal contact with the bottom side of the thermoelectric leg pairs. One or both surfaces often include a system of fins to enhance heat transfer. A portion of the energy transferred to the hot side as heat is directly converted to electrical energy, while the remaining energy is dumped to the coolant. As energy is extracted from the hot fluid and dumped to the cold fluid, the temperature distribution along the length of the system in both the hot and cold fluids will change.

The temperatures of the hot and cold fluids are defined as T_h and T_c respectively and vary with respect to x, the distance along the length of the system; the subscripts h and c will be used generally in what follows to refer to the hot and cold fluids, respectively. The mass flow rates, $\dot{m}$, are defined as being positive for both the hot and cold fluids moving in the positive x-direction (i.e., co-current flow as shown in Fig. 1). The countercurrent configuration is modeled by choosing opposite signs in the mass flow rates. The total rate of energy transferred to all thermoelectric elements in the form of heat is

$$Q_h = (\dot{m}c_p)_h(T_{h,i} - T_{h,o}) \tag{1}$$

where c_p is the heat capacity of the fluid and the subscripts i and o denote the system inlet and outlet temperatures, respectively. The total rate of energy transferred from the thermoelectric elements on the coolant side of the system is

$$Q_c = (\dot{m}c_p)_c(T_{c,o} - T_{c,i}) \tag{2}$$

The electrical power generated by the entire system is the difference in the two energy rates in Eqs. (1) and (2)

$$P = Q_h - Q_c \tag{3}$$

One goal in designing a heat recovery system is often to maximize the electrical power generated, P, compared with the maximum rate of thermal energy available in the waste stream, Q_{max}. The system efficiency quantifies the ratio of the two as

$$\eta_{sys} = P/Q_{max} \tag{4}$$

where

$$Q_{max} = (\dot{m}c_p)_h(T_{h,i} - T_{ambient}) \tag{4b}$$

In Eq. (5), $T_{ambient}$ is the temperature of the local heat sink which is assumed in this paper to be that of the coolant fluid at its inlet to the system, $T_{c,i}$. This definition of system efficiency was also used by Zhou et al. [12]. Note this definition of efficiency is different from the usual definition of efficiency, η, defined as the ratio of the power generated by all leg pairs to the heat absorbed at the hot side of all leg pairs and expressed as

$$\eta = P/Q_h \tag{5}$$

Eq. (5) is appropriate for closed system heat sources such as radioisotope thermoelectric generators. Most waste heat recovery applications are open systems so it is more appropriate to consider the ratio of generated power to thermal power supplied as discussed by Min and Rowe [19]. Eq. (4) is slightly different than defined by Min and Rowe, however; in Eq. (4) the denominator is the thermal power available versus thermal power supplied. The Min and Rowe definition is more appropriate when fuel is being supplied solely for the purposes of thermoelectric power conversion. For applications where waste heat is being tapped, Eq. (4) is most appropriate.

To determine the temperature profiles of the fluids and junction, the thermal transfer at the thermoelectric elements must be examined. Consider a single leg pair as shown in Fig. 2, where the n-type leg is immediately behind p-type leg. The rate of heat transfer to the hot side of the leg pair can be expressed as [5]

$$q_h = \alpha T_1 I + K(T_1 - T_2) - \frac{R_e I^2}{2} \tag{6}$$

where junction temperatures for the hot and cold side of the thermoelectric elements are T_1 and T_2, respectively and also vary with respect to x (Fig. 2). The electrical resistance, R_e, thermal conductance, K, and Seebeck coefficient, α, for the leg pair can be expressed as

$$\begin{aligned} R_e &= \frac{\rho_n l_n}{A_n} + \frac{\rho_p l_p}{A_p} + 2\frac{R_c''}{A_n} + 2\frac{R_c''}{A_p} \\ K &= \frac{k_n A_n}{l_n} + \frac{k_p A_p}{l_p} \\ \alpha &= \alpha_p - \alpha_n \end{aligned} \tag{7}$$

where l is the leg lengths, A is the cross sectional areas of the legs, R_c'' is the electrical contact resistance, ρ is the electrical resistivity of the legs, and k is the thermal conductivity, all of which are assumed to be constant. In Eq. (7) and throughout this paper, the subscripts n and p on any parameter denote an n-type or p-type semiconductor, respectively. It is assumed that the process is at steady state, and the surfaces of each thermoelectric leg are isothermal and that they have constant properties. The Thomson effect can be accounted for by using an integral average Seebeck coefficient as demonstrated by Sandoz-Rosado et al. [21].

A similar expression for the cold side of the junction can be expressed as [5]

$$q_c = \alpha T_2 I + K(T_1 - T_2) + \frac{R_e I^2}{2} \tag{8}$$

The heat transfer to and from the two sides of the leg pair can also be expressed in terms of the temperature differences between the source and sink fluids and thermal resistances between the fluids and thermoelectric junctions as

$$q_h = \frac{T_h - T_1}{R_h} \tag{9a}$$

$$q_c = \frac{T_2 - T_c}{R_c} \tag{9b}$$

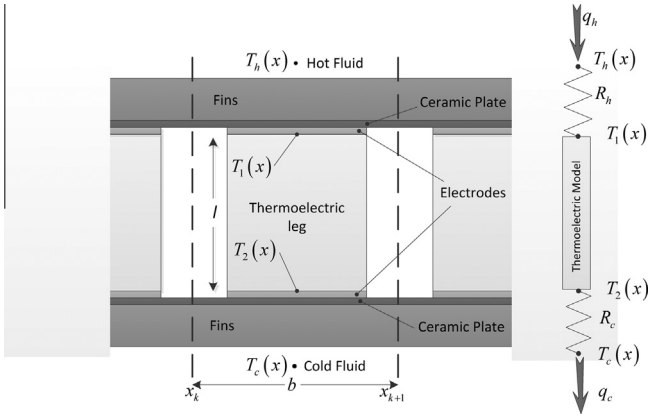

Fig. 2. Schematic of thermoelectric leg with temperature definitions.

where R_h and R_c are the overall thermal resistances between the fluids and thermoelectric junction for a single leg pair. These resistances account for the ceramic layer typically used in modules as well as the fins systems and convection resistances (Fig. 2).

Although there are discrete modules that comprise the thermoelectric system in Fig. 1, we will model the system in such a way that the system can be viewed as a single continuous thermoelectric from which a current can be drawn locally. To this end, we identify a length and width of the thermoelectric leg pair, denoted respectively as b and w, that *extend beyond* the physical length and width of the pair, adding in half of the spaces to the adjacent leg pairs shown in Fig. 2.

We then assume that the length of any leg pair is small compared with the total length of the system, i.e., $b/L \ll 1$, which allows us to view the system as a single continuous module along which the temperatures and current can vary. Consistent with this approximation, we define a local current flux (i.e., current per area), $j(x)$. The current in the kth module can be expressed as:

$$I_k = w\int_{x_k}^{x_{k+1}} j(x)dx \tag{10a}$$

where

$$x_k = (k-1)b, k\epsilon[1, N+1] \tag{10b}$$

In (10b), N is the number of leg pairs. We note that in the limit as $b/L \ll 1$, we can approximate (10) as:

$$I \sim wbj(x) \tag{10c}$$

where the current is now interpreted as being continuous.

In accordance with definition (10b) and the geometry shown in Fig. 2, $L = b{\cdot}N$. To make use of Eq. (10) all parameters and variables are placed on a per area basis, and to this end, Eqs. (6), (8), (9) are written as:

$$q_h'' = \frac{T_h - T_1}{R_h''} = \alpha T_1 j + K''(T_1 - T_2) - \frac{R_e'' j^2}{2} \tag{11a}$$

$$q_c'' = \frac{T_2 - T_c}{R_c''} = \alpha T_2 j + K''(T_1 - T_2) + \frac{R_e'' j^2}{2} \tag{11b}$$

$$p'' = \alpha(T_1 - T_2)j - R_e'' j^2 \tag{11c}$$

where

$$\begin{aligned} R_h'' &= R_h wb \\ R_c'' &= R_c wb \\ R_e'' &= R_e wb \\ K'' &= K/wb \end{aligned} \tag{11d}$$

The heat extracted from the hot fluid and rejected to the cold fluid can be expressed as

$$q_h'' = -(\dot{m}c_p)_h \frac{T_h|_{x_{i+1}} - T_h|_{x_i}}{w(x_{i+1} - x_i)} \tag{12a}$$

$$q_c'' = (\dot{m}c_p)_c \frac{T_c|_{x_{i+1}} - T_c|_{x_i}}{w(x_{i+1} - x_i)} \tag{12b}$$

Combining Eqs. (11) and (12) while considering the limit of $b/L \ll 1$, the following system of equations is obtained

$$\frac{dT_h}{dx} = -C_1(T_h - T_1) \tag{13a}$$

$$\frac{dT_c}{dx} = C_2(T_2 - T_c) \tag{13b}$$

$$T_h - T_1 = D_1 T_1 j + D_2(T_1 - T_2) - D_3 j^2 \tag{13c}$$

$$T_2 - T_c = D_4 T_2 j + D_5(T_1 - T_2) + D_6 j^2 \tag{13d}$$

where

$$\begin{aligned} C_1 &= w/(\dot{m}c_p)_h R_h'' \\ C_2 &= w/(\dot{m}c_p)_c R_c'' \\ D_1 &= \alpha R_h'' \\ D_2 &= K'' R_h'' \\ D_3 &= R_e'' R_h''/2 \\ D_4 &= \alpha R_c'' \\ D_5 &= K'' R_c'' \\ D_6 &= R_e'' R_c''/2 \end{aligned} \tag{13e}$$

In (13e), note that the mass flow rates, $\dot{m}$, are for a *single row* of thermoelectric leg pairs with a width of w, and D_2 and D_5 are the ratios of the fluid-thermoelectric junction resistance to the thermal resistance across the thermoelectric elements. Eq. (13) are subject to the boundary condition $T_h(x = 0) = T_{h,i}$, which is the temperature of the incoming waste heat fluid. The boundary condition for the cold side is either $T_c(x = 0) = T_{c,i}$ for co-current flow or $T_c(x = L) = T_{c,i}$ for countercurrent flow.

Eq. (13) define the temperature profiles for an arbitrary current flux profile, $j(x)$. The power that can be extracted is obtained by subtracting Eq. (11b) from Eq. (11a) and integrating over the entire length of the system to obtain

$$P = w\int_0^L \left[\alpha(T_1 - T_2)j - R_e'' j^2\right]dx \tag{14}$$

Of interest is to maximize the total power generated in accordance with Eq. (14) so that the system efficiency given by Eq. (4) is maximized; this is obtained by determining an optimal current flux profile, $j(x)$. The determination of this current flux is described in the next section.

3. Power optimization—the theoretical limit model

The appearance of the current density in the integral expression for the power, Eq. (14), suggests that a variational method may be used to maximize the power. To this end, we rewrite Eqs. (13c,d) to obtain two explicit expressions for $T_1(x)$ and $T_2(x)$ in terms of $T_h(x)$, $T_c(x)$ and $j(x)$ as

$$T_1(x) = \frac{D_2 T_c + (1 + D_5)T_h - D_4 j T_h + (D_2 D_6 + D_3 D_5 + D_3)j^2 - D_3 D_4 j^3}{(1 + D_2 + D_5) + (D_1 D_5 - D_2 D_4 + D_1 - D_4)j - D_1 D_4 j^2} \tag{15a}$$

$$T_2(x) = \frac{D_5 T_h + (1 + D_2)T_c + D_1 j T_c + (D_2 D_6 + D_3 D_5 + D_6)j^2 + D_1 D_6 j^3}{(1 + D_2 + D_5) + (D_1 D_5 - D_2 D_4 + D_1 - D_4)j - D_1 D_4 j^2} \tag{15b}$$

The total power in Eq. (14) is thus seen to be a function of $T_h(x)$, $T_c(x)$ and $j(x)$. We need to maximize the power, P in Eq. (14), subject to constraints imposed by Eqs. (13a) and (13b). To do so, a Lagrangian function ψ is constructed based on the integrand from the power expression (14), Eqs. (13a) and (13b), and x-dependent Lagrange multipliers $\lambda_1(x)$ and $\lambda_2(x)$ to yield: [22]

$$\begin{aligned} \psi = &\left[\alpha(T_1 - T_2)j - R_e'' j^2\right] + \lambda_1(x)\left[T_h' + C_1(T_h - T_1)\right] \\ &+ \lambda_2(x)\left[T_c' - C_2(T_2 - T_c)\right] \end{aligned} \tag{16}$$

where $T_h' = \frac{dT_h}{dx}$ and $T_c' = \frac{dT_c}{dx}$. By inspection, we see that when the constraints given in Eqs. (13a) and (13b) are satisfied, the terms multiplying the Lagrange multipliers are zero, and the power is given as

$$P = w\int_0^L \psi dx \tag{17}$$

Optimization of the functional, ψ, with respect to the three functions $T_h(x), T_c(x)$ and $j(x)$, yields the well-known Euler–Lagrange equations [22]; system specific boundary conditions are

necessary to eliminate boundary terms arising through the standard integration by parts in the derivation of the equations [22]. These equations and constraints are given as:

$$\begin{aligned}
&\frac{\partial \psi}{\partial j} = 0 \\
&\frac{\partial \psi}{\partial T_h} - \frac{d}{dx}\left(\frac{\partial \psi}{\partial T_h'}\right) = 0 \\
&\frac{\partial \psi}{\partial T_c} - \frac{d}{dx}\left(\frac{\partial \psi}{\partial T_c'}\right) = 0 \\
&@\, x = 0, \quad \frac{\partial \psi}{\partial T_c'} = 0 \\
&@\, x = L, \quad \frac{\partial \psi}{\partial T_h'} = 0
\end{aligned} \tag{18}$$

The substitution of Eq. (16) into Eq. (18) yields the following

$$\begin{aligned}
&\alpha j\left(\frac{\partial T_1}{\partial j} - \frac{\partial T_2}{\partial j}\right) + \alpha(T_1 - T_2) - 2jR_e'' - C_1\lambda_1\frac{\partial T_1}{\partial j} - C_2\lambda_2\frac{\partial T_2}{\partial j} = 0 \\
&\alpha j\left(\frac{\partial T_1}{\partial T_h} - \frac{\partial T_2}{\partial T_h}\right) + \lambda_1\left[C_1 - C_1\frac{\partial T_1}{\partial T_h}\right] - C_2\lambda_2\frac{\partial T_2}{\partial T_h} - \frac{d\lambda_1}{dx} = 0 \\
&\alpha j\left(\frac{\partial T_1}{\partial T_c} - \frac{\partial T_2}{\partial T_c}\right) + \lambda_2\left[C_2 - C_2\frac{\partial T_2}{\partial T_c}\right] - C_1\lambda_1\frac{\partial T_1}{\partial T_c} - \frac{d\lambda_2}{dx} = 0
\end{aligned} \tag{19a}$$

with the following boundary conditions.

$$@\, x = 0, \quad T_h = T_{h,\text{in}}, \quad \lambda_2 = 0\,; \quad @\, x = L, \quad T_c = T_{c,\text{in}}, \quad \lambda_1 = 0. \tag{19b}$$

The set of nonlinear Eq. (19), coupled with Eqs. (13) and (15), represent a system of 5 equations in the 5 unknown functions: $T_h(x)$, $T_c(x)$, $j(x)$, $\lambda_1(x)$ and $\lambda_2(x)$; this system is solved using a full Newton's iteration method. Sufficient accuracy is obtained with 400 equally spaced discretizations along x for each variable. The coupled system is solved iteratively until both the Euclidean norm of the equation residuals and that of the change to all dependent variables is less than 10^{-8}.

In the case of co-current flow, the boundary conditions in the system (19) switch location in such a way that there are two boundary conditions at each end of the computational domain. The boundary conditions for co-current flow are

$$@\, x = 0, \quad T_h = T_{h,\text{in}}, \quad T_c = T_{c,\text{in}}; \quad \text{and} \quad @\, x = L, \quad \lambda_1 = 0, \quad \lambda_2 = 0 \tag{19c}$$

For purposes of discussion, we will refer to the above described approach as the Theoretical Limit Model.

4. Results and discussion

We now examine results of the theoretical limit model. To do so, we specify some typical properties (Table 1) and system level parameters (Table 2) that will be used for all examples in the rest of this paper, except where noted. With this initial specification, we consider a waste heat recovery application with an exhaust temperature of 500 °C and mass flow rate of 25 g/s (these values indicated in Table 2). The system is to be cooled in a counter flow configuration by a coolant at 50 °C with a heat capacity rate, $\dot{m}c_p$, ten times that of the exhaust side.

In Table 2, we have adhered to the naming convention that a module corresponds to multiple leg pairs (modules are how thermoelectric are used in practice); however, note that it is the performance of each leg pair in the system that is being examined in our work. The model developed in Sections 2 and 3 is used to extract the optimal current flux profile, $j(x)$, that should be applied to the system to maximize output power and therefore overall system efficiency defined in Eq. (4); Fig. 3 shows the profile of the current in accordance with Eq. (10c) for the thermoelectric module. Fig. 4 provides the corresponding temperature profiles along the module. These figures indicate that the current is greatest where the largest temperature differences exist across the leg pairs. For this particular system, a maximum power of 390 W is reached with an overall system efficiency of 3.4% as defined by Eq. (4). This overall efficiency is significantly less than the leg pair efficiency of 6.7%, defined by Eq. (5). A similar simulation for the co-current flow configuration generates very similar results owing to the high heat capacity rate of the coolant, $(\dot{m}c_p)_c$.

A reduction of the heat capacity ratio, $(\dot{m}c_p)_c/(\dot{m}c_p)_h$, from ten to three and one, results in smaller temperature differences and therefore power generation, given by 350 W and 261 W, respectively. In the latter case, the temperature difference across the legs and current is nearly constant across the entire system.

Fig. 5 shows that the addition of thermoelectric modules, each consisting of 127 leg pairs, to a system will not always increase power. In fact, for the parameters of Tables 2 and 3, the power peaks at around 490 W for approximately 65 modules. Beyond this amount, an increase in the number of modules results in a negligible increase in generated power due to a decrease in the average temperature difference in the system leg pairs over the length of

Table 1
Leg pair parameters.

Parameters	p type	n type
Seebeck coefficient, α	$200{\cdot}10^{-6}$ V/K	$-150{\cdot}10^{-6}$ V/K
Electrical resistivity, ρ	$1.5{\cdot}10^{-3}$ Ω cm	$2.0{\cdot}10^{-3}$ Ω cm
Thermal conductivity, k	1.1 W/m K	1.3 W/m K
Leg length, l	1 mm	1 mm
Leg area, A	2.25 mm^2	2.25 mm^2
Electrical contact resistance, R_c''	0 Ω m^2	0 Ω m^2

Table 2
Other system parameters.

Exhaust inlet temperature, $T_{h,in}$	500 °C
Coolant inlet temperature, $T_{c,in}$	50 °C
Exhaust mass flow rate, $\dot{m}$	25 g/s
Coolant heat capacity ratio to exhaust heat capacity ratio, $(\dot{m}c_p)_c/(\dot{m}c_p)_h$	10
# Leg pairs per module	127
# Modules in system	25
Ratio of hot side external resistance to internal thermal resistance, $K''R_h''$	0.1
Ratio of cold side external resistance to internal thermal resistance, $K''R_c''$	0.1

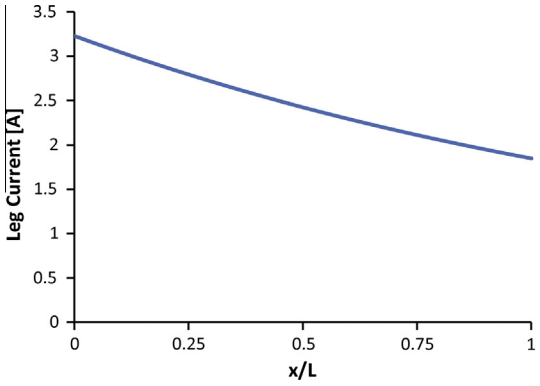

Fig. 3. Leg current, I, along the length of system in accordance with Eq. (10c).

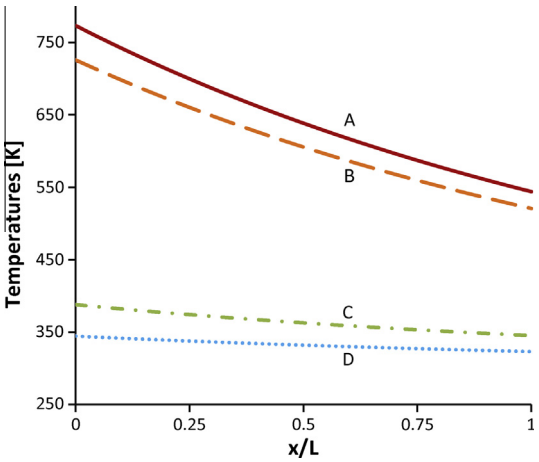

Fig. 4. Temperature profile for the current profile shown in figure. (A) T_h, (B) T_1, (C) T_2, and (D) T_c.

the system. For the situation where the heat capacity rate of the coolant is three times that of the exhaust heat capacity rate, the output power decreases with the addition of modules at some point. Presumably, this occurs because adding more modules results in parasitic heat losses due to conduction through the added modules. The peak power for this reduced coolant heat capacity rate is 400 W with 40 modules.

The relative resistances of the system heat sinks have a significant impact on overall system performance. The results presented above were for the case where the ratio of thermal resistances for the heat sinks on both the hot and cold sides of the system to the module thermal resistance, $K''R_h''$ and $K''R_c''$, are 0.1. Increasing the resistance ratio to 0.5 while holding all other variables constant (again, those in Tables 2 and 3) results in 154 W generated, a 60% decrease in power generated. This result indicates that close attention is needed to the design of the heat sinks in any waste heat recovery systems.

Although ZT, the thermoelectric figure of merit, is often used to compare potential thermoelectric materials, it is not sufficient in open heat recovery systems consisting of many modules. For example, if the electrical resistivity is decreased and the thermal conductivity is increased by a factor of two and all other system parameters are held fixed, the output power decreases from 390 W to 381 W despite the fact that ZT is unchanged. Similarly

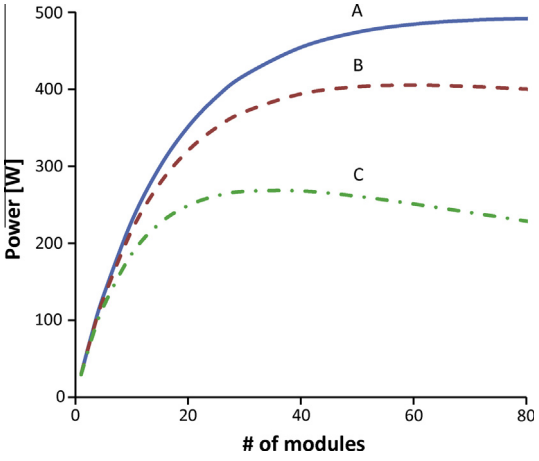

Fig. 5. Optimal power versus number of modules in system for three different heat capacity ratios where (A) $(\dot{m}c_p)_c/(\dot{m}c_p)_h = 10$, (B) $(\dot{m}c_p)_c/(\dot{m}c_p)_h = 3$, and (C) $(\dot{m}c_p)_c/(\dot{m}c_p)_h = 1$.

Table 3
Ranges of system configurations considered.

$(\dot{m}c_p)_c/(\dot{m}c_p)_h$	1, 3, 10
# Modules in system	1, 5, 25, 50
$K''R''$	0.01, 0.1, 0.5
k_p & k_n (W/m K)	1.1 & 1.3, 1/3•(1.1) & 1/3•(1.3)

if we increase the electrical resistance and decrease thermal conductivity by a factor of two, the output power generated decreases to 320 W even though the ZT is the same for both cases. Therefore, ZT alone is not a sufficient metric for comparing materials options for open heat recovery systems.

4.1. Alternative optimization approaches

Three alternative approaches have been used in the literature to optimize systems having multiple thermoelectric leg pairs, and it is judicious to compare results with those of the theoretical limit model. The three approaches used are: (1) to optimize local efficiency across each thermoelectric leg pair [19], (2) to fix the voltage across all leg pairs to optimize the overall system power by adjusting the single voltage across each leg pair [18], and (3) to string all legs in series and optimize power for a single operating current [16,17]. The latter two approaches are simpler to implement than the former in real systems. None of these alternatives will necessarily guarantee the maximum system efficiency as defined by Eq. (4). What follows is the formulation of the equations required for the system optimization using these modeling approaches, followed by a comparison with the theoretical limit model developed in Sections 2 and 3. All notation used is as defined previously.

4.2. Optimization by local efficiency

Following the approach of Refs. [5,19], the efficiency across a single leg can be optimized by the following expression for current flux

$$j_{max} = \frac{\alpha(T_1 - T_2)}{R_e''(1+m)} \tag{20a}$$

$$\text{where } m = \sqrt{1+z\overline{T}}; \quad z = \frac{\alpha^2}{K''R_e''} \text{ and } \overline{T} = \frac{(T_1+T_2)}{2} \tag{20b}$$

We augment this cited work, however, by including thermal resistance between the fluids and thermoelectric junctions, which have already been included in Eq. (11) and illustrated schematically in Fig. 2. After substitution of j_{max} into Eq. (11), the results are

$$q_h'' = \frac{T_h - T_1}{R_h''} = \alpha^2 T_1 \frac{(T_1 - T_2)}{R_e''(1+m)} + K''(T_1 - T_2) - \frac{\alpha^2(T_1 - T_2)^2}{2R_e''(1+m)^2} \tag{21a}$$

$$q_c'' = \frac{T_2 - T_c}{R_c''} = \alpha^2 T_2 \frac{(T_1 - T_2)}{R_e''(1+m)} + K''(T_1 - T_2) + \frac{\alpha^2(T_1 - T_2)^2}{2R_e''(1+m)^2} \tag{21b}$$

Eq. (21) are divided by K'' and rewritten in terms of z according to Eq. (20b) to yield the following

$$\frac{T_h - T_1}{D_2} = zT_1 \frac{(T_1 - T_2)}{(1+m)} + (T_1 - T_2) - \frac{z(T_1 - T_2)^2}{2(1+m)^2} \tag{22a}$$

$$\frac{T_2 - T_c}{D_5} = zT_2 \frac{(T_1 - T_2)}{(1+m)} + (T_1 - T_2) + \frac{z(T_1 - T_2)^2}{2(1+m)^2} \tag{22b}$$

where

$$D_2 = R_h''K'' \text{ and } D_5 = R_c''K'' \tag{22c}$$

The set of nonlinear Eq. (22), coupled with the differential Eqs. (13a) and (13b) and their corresponding boundary conditions for co- or counter-current flows (given respectively by Eqs. (19a) and (19b)), are well posed to solve for the temperature field and the current flux. We solve the system using a full Newton's iteration in a similar way to that described in Section 3. Once solved, the power is determined as:

$$P = w\int_0^L (q_h'' - q_c'')dx = w\int_0^L \left(\frac{T_h - T_1}{R_h''} - \frac{T_2 - T_c}{R_c''}\right)dx \tag{23}$$

The model described above will be referred to as the Local Efficiency Optimization Model.

4.3. Optimization for fixed voltage

For the case where the voltage, V, is the same for each leg pair, the current flux is expressed as

$$j = \frac{\alpha(T_1 - T_2)}{R_e''} - \frac{V}{R_e''} \tag{24}$$

The total power can then be extracted as

$$P = w\int_0^L jV dx = \frac{wV\alpha}{R_e''}\int_0^L (T_1 - T_2)dx - \frac{wV^2L}{R_e''} \tag{25}$$

The maximum power is achieved when $\frac{dP}{dV} = 0$, which yields

$$V = \frac{\alpha}{2L}\int_0^L (T_1 - T_2)dx \tag{26}$$

An expression for current flux, j_{max}, that maximizes the power is obtained after substitution of Eq. (26) into Eq. (24) to yield

$$j_{max} = \frac{\alpha}{R_e''}[(T_1 - T_2) - T^*] \tag{27a}$$

$$\text{where } T^* = \frac{1}{2L}\int_0^L (T_1 - T_2)dx \tag{27b}$$

Upon substitution of Eq. (27) into Eq. (11), dividing by K″, and simplifying, the result is

$$\frac{T_h - T_1}{D_2} = (T_1 - T_2) + z\left(\overline{T} + \frac{T^*}{2}\right)[(T_1 - T_2) - T^*] \tag{28a}$$

$$\frac{T_2 - T_c}{D_5} = (T_1 - T_2) + z\left(\overline{T} - \frac{T^*}{2}\right)[(T_1 - T_2) - T^*] \tag{28b}$$

$$\text{where } z = \frac{\alpha^2}{K''R_e''}, \quad D_2 = R_h''K'', \; D_5 = R_c''K'' \text{ and } \overline{T} \text{ given in eq. (20b)} \tag{28c}$$

Eq. (28), coupled with the differential Eqs. (13a) and (13b) and their corresponding boundary conditions for co- or counter-current flows (given by Eqs. (19a) and (19b), respectively), are well posed to solve for the temperature field and the current flux. Once solved, the power is extracted by combining Eqs. (25) and (26) to yield

$$P = \frac{wLV^2}{R_e''} \tag{29}$$

where V is given by Eq. (26). The system is solved using a full Newton's iteration in a similar way to that described in Section 3. For purposes of later discussion, we denote the above model as the Constant Voltage Optimization Model.

4.4. Optimization via constant current

For a fixed constant current, Eq. (13) are solved directly, and the power is extracted from Eq. (14). An inverse parabolic method is used to optimize the power with respect to current flux. This is obtained by imposing a current, solving the system (13), calculating the power (14), and then repeating this process by systematically changing the current to find the highest power. This model is referred to as the Constant Current Optimization model in what follows.

4.5. Comparison of optimization approaches

The temperature and current profiles for the parameter values in Tables 1 and 2 are shown in Figs. 6 and 7. The profile for the theoretical limit model developed in Sections 2 and 3 is also included.

For this particular case, the system efficiency for the theoretical limit model is only 0.1% greater than that of the local efficiency optimization model, while the local efficiency optimization model has a 0.3% greater module efficiency as defined by Eq. (5). This negligible difference was common for the wide range of system configurations defined in Table 3.

Differences increase between the local efficiency optimization model and the theoretical limit model as the ratio of hot side external resistance to internal thermal resistance, $K''R''$; thermal conductivity, k; and number of modules, N, decrease. For a case where $K''R_h'' = K''R_c'' = 0.01$ and k is decreased by a factor of three from the base case, the local optimization model yields a total system efficiency that is 2.7% below that of the theoretical limit model. With the exception of systems with one and five modules, $K''R_h'' = K''R_c'' = 0.01$ and k is decreased by a factor of three from the base case, the differences between the two models were less than 3% and in most cases less than 1%. No case defined by the permutations in Table 3 resulted in differences greater than 8%.

The differences between the theoretical limit model and the voltage optimization model are more pronounced and can be quite significant in some cases. For the parameter values in Tables 1 and 2, the constant voltage optimization model results yields nearly 6% less power than that from the theoretical limit model. This difference increases dramatically as more modules are added to the system as shown in Fig. 8 or when operating the system in a co-current configuration. For example, a system with 50 modules will deliver 16% less energy for a constant voltage condition versus the theoretical limit for a counter flow configuration; by contrast, a co-current system with 50 modules for the same conditions results in a nearly a 28% difference. Differences are also more significant for lower mass flow rates and when a large portion of the thermal energy is removed from the exhaust stream. Although it is simple

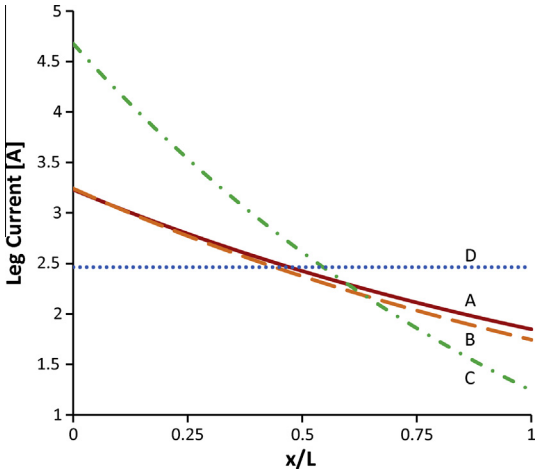

Fig. 6. Current profile along the length of system. (A) theoretical limit model, (B) local efficiency optimization model, (C) constant voltage optimization model, and (D) constant current optimization model.

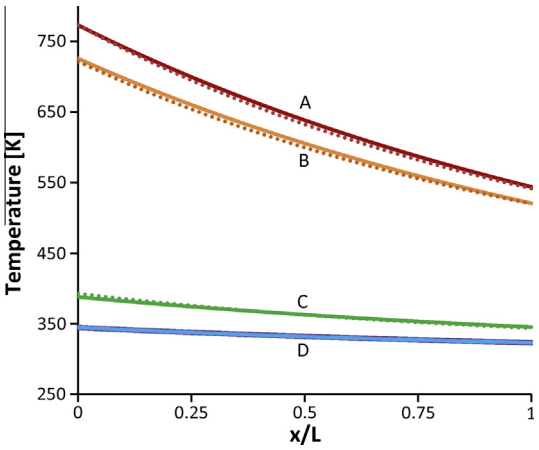

Fig. 7. Temperature profile for the current profile shown in Fig. 5. (A) T_h, (B) T_1, (C) T_2, and (D) T_c. Solid lines are for theoretical limit model and dotted lines are for constant voltage optimization model. Local efficiency optimization model results are indistinguishable from theoretical limit curves.

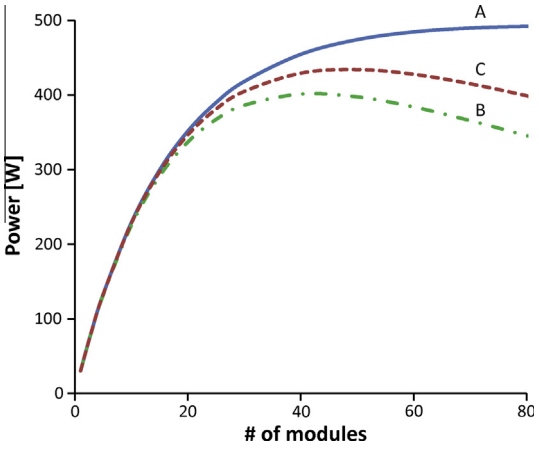

Fig. 8. Power versus number of modules for counter flow systems with constant voltage and constant current models compared to the theoretical limit with system parameters defined in Tables 1 and 2. (A) theoretical limit and local efficiency optimization approach (indistinguishable on scale of plot), (B) constant voltage approach and (C) constant current approach.

to implement a single fixed voltage across the entire system in practice, the loss in overall performance can be significant.

Fig. 8 shows that optimal power predictions can differ significantly between the theoretical limit model and the constant current optimization model as the number of modules increase; however, the differences are much more pronounced for the constant voltage optimization model. For the parameter values in Tables 1 and 2, the constant current optimization model results yields more than 2% less power that from the theoretical limit model.

5. Conclusions

The theoretical limit of the maximum power that can be extracted from a thermoelectric system in contact with a hot exhaust stream has been determined using a variational method. The limit is determined from a computationally efficient optimization algorithm for co- and counter-current flow configurations used in waste heat recovery systems. The theoretical limit model predicts that there is an optimum number of thermoelectric modules that maximize the power extracted for any system, and that adding more modules beyond this optimum can actually degrade system performance. Three different electric loading approaches found in the literature were compared to the theoretical limit using typical parameter values corresponding to automobile exhaust—optimization of local thermoelectric efficiency, optimization of power for fixed current, and optimization of power for fixed voltage. It is found that in most cases, optimization of local thermoelectric efficiency leads to predictions close to that of the theoretical limit; deviations arise, however, in situations of high heat transfer resistances in the fluids. For cases where little thermal energy is extracted from the exhaust gases, power optimization approaches employing either constant voltage or constant current assumptions predict optimal system power near the theoretical limit. For cases where a significant portion of the thermal energy is utilized to generate power, wiring thermoelectric leg pairs in series (constant current) results in higher system efficiencies compared to cases where the leg pairs are wired in parallel (constant voltage). This work demonstrates that the thermoelectric figure of merit alone is not sufficient to fully characterize the efficiency of a system. Other system parameters, included in the theoretical limit algorithm, are necessary to fully characterize the theoretical system limit.

Due to its low computational load, the theoretical limit model could be imbedded in the design of a thermoelectric system; in practice however, its implementation would require the use of a relatively sophisticated control scheme to assure predicted current loading. The utility of the model, however, is not limited to this use, as it provides a theoretical limit against which the power drawn from simpler configurations and control schemes may be compared. This allows engineers to make judgments on the benefits and costs of simpler, application-specific configurations, trading off complexity (and thus cost and robustness) with the loss of power. For example, based on the case study considered and shown in Fig. 8, one can conclude that the power obtained from a system of up to 30 modules, run under a constant current scenario, is approximately that of the theoretical maximum. Thus, an engineer would no doubt choose the simpler constant current implementation approach in an application where 30 modules produce the desired level of power.

References

[1] Yang J. Potential applications of thermoelectric waste heat recovery in the automotive industry. In: ICT 2005. 24th int. conf. thermoelectr., IEEE; 2005. p. 170–4.
[2] Hendricks T, Choate WT. Engineering scoping study of thermoelectric generator systems for industrial waste heat recovery. U.S. Department of Energy: Industrial Technologies Program; 2006.
[3] Alam H, Ramakrishna S. A review on the enhancement of figure of merit from bulk to nano-thermoelectric materials. Nano Energy 2013;2:190–212.
[4] Chen Z-G, Han G, Yang L, Cheng L, Zou J. Nanostructured thermoelectric materials: current research and future challenge. Prog Nat Sci Mater Int 2012;22:535–49.
[5] Angrist SW. Direct energy conversion. 4th ed. Boston, MA: Allyn and Bacon, Inc.; 1982.
[6] Snyder GJ, Ursell TS. Thermoelectric efficiency and compatibility. Phys Rev Lett 2003;91:148301.
[7] Anatychuk LI, Kuz RV. Materials for vehicular thermoelectric generators. J Electron Mater 2012;41:1778–84.
[8] Miller EW, Hendricks TJ, Wang H, Peterson RB. Integrated dual-cycle energy recovery using thermoelectric conversion and an organic Rankine bottoming cycle. Proc Inst Mech Eng Part A J Power Energy 2011;225:33–43.
[9] Yazawa K, Koh YR, Shakouri A. Optimization of thermoelectric topping combined steam turbine cycles for energy economy. Appl Energy 2013;109:1–9.
[10] Sahin aZ, Yilbas BS, Shuja SZ, Momin O. Investigation into topping cycle: thermal efficiency with and without presence of thermoelectric generator. Energy 2011;36:4048–54.
[11] Gao X, Andreasen SJ, Chen M, Kær SK. Numerical model of a thermoelectric generator with compact plate-fin heat exchanger for high temperature PEM fuel cell exhaust heat recovery. Int J Hydrogen Energy 2012;37:8490–8.

[12] Zhou S, Sammakia BG, White B, Borgesen P. Multiscale modeling of thermoelectric generators for the optimized conversion performance. Int J Heat Mass Transf 2013;62:435–44.
[13] Yu J, Zhao H, Jianlin Y, Hua Z. A numerical model for thermoelectric generator with the parallel-plate heat exchanger. J Power Sources 2007;172:428–34.
[14] Kumar S, Heister SD, Xu X, Salvador JR, Meisner GP. Thermoelectric generators for automotive waste heat recovery systems part ii: parametric evaluation and topological studies. J Electron Mater 2013;42:944–55.
[15] Kumar S, Heister SD, Xu X, Salvador JR, Meisner GP. Thermoelectric generators for automotive waste heat recovery systems part I: numerical modeling and baseline model analysis. J Electron Mater 2013;42:665–74.
[16] Crane DT. An introduction to system-level, steady-state and transient modeling and optimization of high-power-density thermoelectric generator devices made of segmented thermoelectric elements. J Electron Mater 2010;40:561–9.
[17] Wang Y, Dai C, Wang S. Theoretical analysis of a thermoelectric generator using exhaust gas of vehicles as heat source. Appl Energy 2013;112:1–10.
[18] Liang G, Zhou J, Huang X. Analytical model of parallel thermoelectric generator. Appl Energy 2011;88:5193–9.
[19] Min G, Rowe DM. Conversion efficiency of thermoelectric combustion systems. Energy Convers, IEEE Trans 2007;22:528–34.
[20] Ioffe AF. Semiconductor thermoelements and thermoelectric cooling. London: Infosearch; 1957.
[21] Sandoz-Rosado EJ, Weinstein SJ, Stevens RJ. On the Thomson effect in thermoelectric power devices. Int J Therm Sci 2013;66:1–7.
[22] Liberzon D. Calculus of variations and optimal control theory. Oxfordshire: Princeton University Press; 2012.